

## AERODYNAMIC CHARACTERISTICS OF A SIX BLADED SAVONIUS ROTOR

Shamsun Nahar, Md. Quamrul Islam and Mohammad Ali

Mechanical Engineering Department, Bangladesh University of Engineering and Technology (BUET)

### ABSTRACT

The research work has been carried out to study the aerodynamic characteristic i.e., drag coefficient torque coefficient etc. of a vertical-axis six bladed Savonius rotor. The pressure measurements have been made at 26 tapping points on each blade of the vane rotor. Pressure on the convex and concave surfaces have been measured for every  $10^\circ$  interval of rotor angle up to  $360^\circ$  angle of rotation. To calculate drag force and torque in non-dimensional form, computer based software has been used and the output has been subsequently plotted and analyzed. The effects of individual blade and also the combined effects of six blades on different aerodynamic characteristics are analyzed in this research work.

A quasi-steady approach has been applied for the prediction of the dynamic performance of the rotor using the static drag and torque coefficients. Power coefficient versus tip speed ratio curve for six bladed Savonius rotor has been drawn.

**Keywords:** Drag Coefficient, Torque Coefficient, Wind Turbines.

### 1. INTRODUCTION

The science of exploitation of wind power is not a new one. For the past few centuries people are extracting energy from the wind in various ways. One means for converting wind energy to a more useful form is through the use of windmills. Recently, due to the fuel crisis, this science is gaining more popularity. Wind energy has become very lucrative now-a-days due to its reliability. The European Wind Energy Association (EWEA) estimates that between, 20 GW and 40 GW of offshore wind energy capacity will be operating in the European Union by 2020. A fully developed European offshore wind resources could deliver a capacity of several hundred GW keen interest to develop efficient and economic devices to collect energy from the wind. Recently the utilization of wind power is increasing in many developed as well as under developed countries. There are various types of windmills. The most common one having the blades of airfoil shape is the horizontal axis wind turbine. Another type is the vertical axis wind turbine is the simplicity of its manufacture compared to horizontal axis wind turbine. Among the different vertical axis wind turbines, the Savonius rotor is a slow running wind machine and has a relatively lower efficiency. Still it is being used in the developing countries because of its simple design, easy and cheap technology for construction and a good starting torque independent of wind direction at low wind speeds [1, 2, 3]. Rigorous studies on the performance characteristics of the Savonius rotor are found in the literatures and these enable the identification of an optimum geometrical configuration for practical design [4, 5, 6, 7, 8].

### 2. THE SIX BLADED SAVONIUS ROTOR

The Savonius rotor was made up of three half cylinders (blade) of diameter,  $d=106$  mm and height  $H=300$ mm. The cylinders were made of PVC material. The overlap distance  $S$  was selected to be one fifth of the cylinder diameter (i.e.,  $S=a/d=0.3$ ) and the central shaft had been removed. The overlap distance selected was the optimum value with respect to the wind power extraction. The whole rotor was fixed on an iron frame by using two side shafts and two ball bearings. The pressure measurements were made at 26 pressure tapping points on each blade.

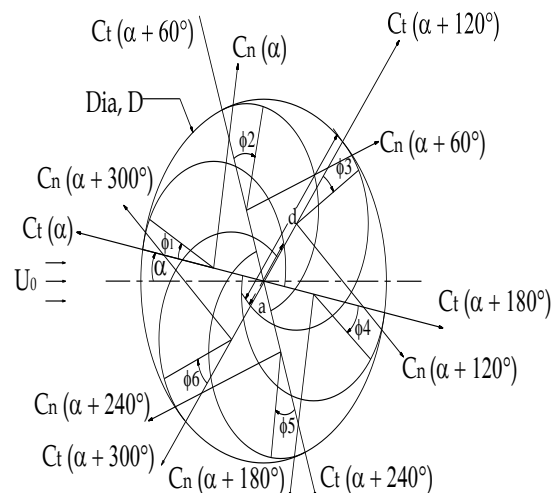


Fig 1. Forces acting on blades

The tappings were made with copper tubes of 1.5mm outer diameter and 10mm length which were press fitted to the tapping holes. The tappings were located at the mid-plane of one side of each blade, so that pressure distribution at every 10° on the blade surface could be measured. The pressure tappings were connected to a inclined multimanometer (manometric fluid was water and had an accuracy of ± 0.1 mm of water column) through 2mm PVC tubes. The pressures were measured at every 10° interval of rotor angle so that a detailed picture of the aerodynamic loading and torque characteristics could be obtained.

1. Converging mouth entry
2. Perspex section
3. Rectangular diverging section
4. Fan section
5. Butter fly section
6. Silencer with honey comb section
7. Diverging section
8. Converging section
9. Rectangular section
10. Flow straightner section
11. Rectangular exit section

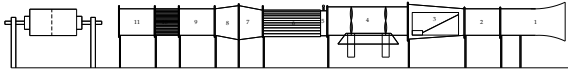


Figure 2: Schematic diagram of wind tunnel



Fig 3. Set-up of Experiment

## 2.1 Pressure Co-efficient, $C_p$

Pressure coefficient is defined as

$$C_p = \frac{P - P_0}{\frac{1}{2}\rho U_0^2} \quad (1)$$

Where,  $P - P_0$  = Difference between blade and atmospheric pressure in pascal

$\rho$  = Density of air

$U_0$  = Free stream velocity

## 2.2 Drag Coefficient

The drag coefficients in normal and tangential directions can be written as follows:

$$C_n = \frac{F_n}{\frac{1}{2}\rho U_0^2 d}$$

$$C_t = \frac{F_t}{\frac{1}{2}\rho U_0^2 d} \quad (2)$$

To obtain the drag coefficients in the normal and tangential direction of the chord, the values of  $F_n$  and  $F_t$  must be known beforehand. The values of the forces  $F_n$  and  $F_t$  are obtained by integrating the pressure for a blades as follows:

$$F_n = \int_0^\pi \Delta P \frac{d}{2} \cos \phi d\phi = \sum_{i=1}^{26} \Delta P_i \frac{d}{2} \cos \phi_i \Delta \phi_i \quad (3)$$

and similarly

$$F_t = \sum_{i=1}^{26} \Delta P_i \frac{d}{2} \sin \phi_i \Delta \phi_i$$

Where  $\Delta P_i$  is the difference in pressure on the concave and convex surfaces at particular pressure tapping,  $i$ .

Where  $F_n$  is responsible for producing a torque on the shaft of the rotor and this torque can be expressed for a blade as

Torque on a blade,

$$\begin{aligned} T &= F_n \times \frac{d-a}{2} \\ &= F_n \times \frac{d}{2} \left(1 - \frac{a}{d}\right) \\ &= F_n \times \frac{d}{2} \times (1-s) \end{aligned} \quad (4)$$

## 2.3 Torque Coefficient

Equation (4) can be reduced to get the torque coefficient for a single blade at a particular rotor angle as

$$\begin{aligned} C_q(\alpha) &= \frac{F_n}{\frac{1}{2}\rho U_0^2} \times \frac{(d-a)}{2} \times \frac{2}{2d-a} \\ &= C_n(\alpha) \times \frac{d-a}{2d-a} \\ &= C_n(\alpha) \times \frac{d(1-a/d)}{d(2-a/d)} \end{aligned}$$

$$C_q(\alpha) = C_n(\alpha) \frac{(1-s)}{(2-s)} \quad (5)$$

The total static torque coefficient produced on the rotor shaft by the six blades can be expressed as follows:

$$C_Q = \frac{(F_{n1} + F_{n2} + F_{n3})}{\frac{1}{2}\rho U_0^2} \times \frac{\frac{(d-a)}{2}}{\frac{(2d-a)}{2}}$$

$$= \frac{(F_{n1} + F_{n2} + F_{n3})}{\frac{1}{2} \rho U_0^2} \times \frac{d-a}{2d-a} \times \frac{d}{D}$$

$$C_Q = [C_n(\alpha) + C_n(\alpha + 60^\circ) + C_n(\alpha + 120^\circ) + C_n(\alpha + 180^\circ) + C_n(\alpha + 240^\circ) + C_n(\alpha + 300^\circ)] \times 1 - s_2 - s_2 \quad (6)$$

Where  $C_n(\alpha)$ ,  $C_n(\alpha + 60^\circ)$ ,  $C_n(\alpha + 120^\circ)$ ,  $C_n(\alpha + 180^\circ)$ ,  $C_n(\alpha + 240^\circ)$ , and  $C_n(\alpha + 300^\circ)$  refer to the drag coefficients of the first, second, third, fourth, fifth and sixth blade respectively at rotor angle  $\alpha$ .

Power coefficient at  $\alpha$ ,

$$C_p(\alpha) = C_Q'(\alpha) \cdot \lambda$$

A computer programme was performed to calculate the power coefficient ( $C_p$ ) using the value of the component of relative velocity  $V_w$  along  $U_0$  and static normal drag coefficient  $C_n(\alpha)$  for three different tip speed ratio  $\lambda$  with the help of equations (7) to (14). The program output gave three sets of dynamic torque coefficients and power coefficient and finally three average value of power coefficient  $C_{pave}$ .

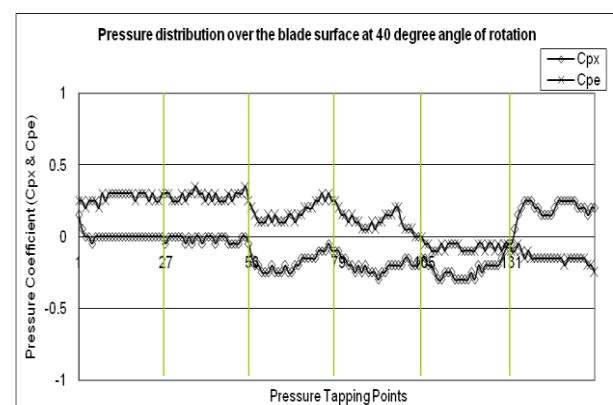
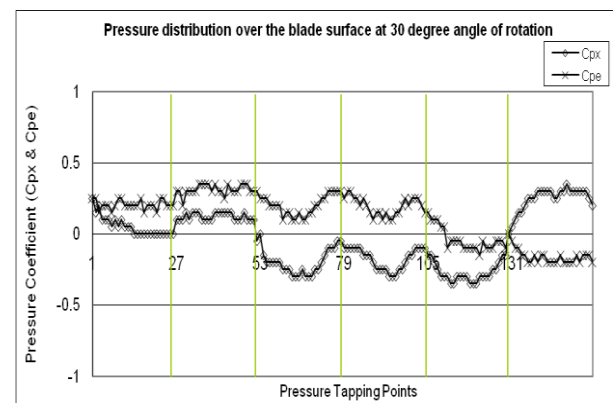
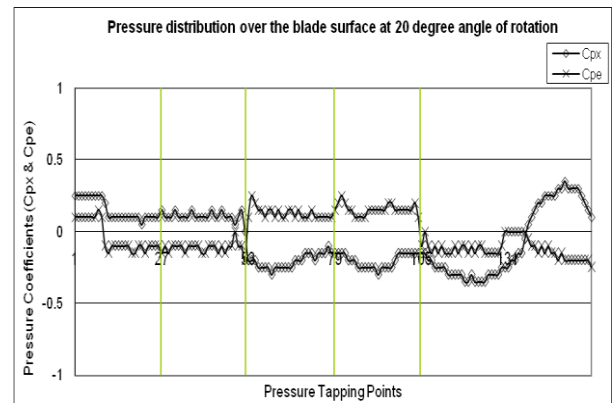
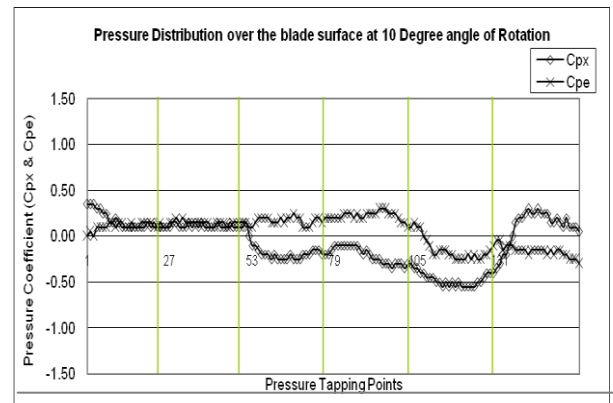
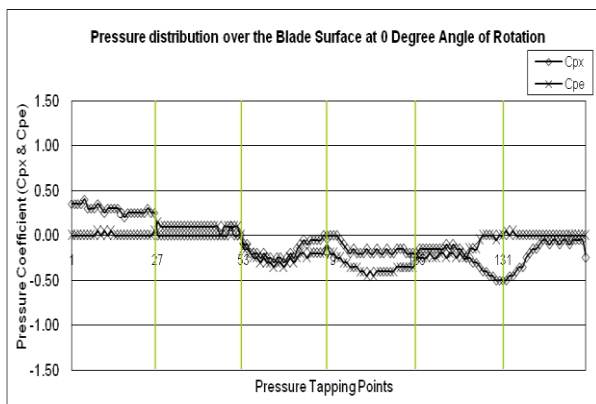
Power coefficient vs. tip speed ratio of the present prediction and the previous researchers prediction were plotted on the same graph for analysis.

### 3. RESULTS AND DISCUSSION

The results of experimental investigation conducted for the wind tunnel flow over the six bladed Savonius rotor. The results of the pressure distribution over the convex and concave surfaces of each blade at different angle of rotation are analyzed first. Nature of the drag and static torque characteristics are also analyzed. This topic includes the analysis of pressure distribution, normal drag coefficient ( $C_n$ ), tangential drag coefficient ( $C_t$ ), torque coefficient ( $C_q$ ), and total static torque coefficient ( $C_Q$ ).

#### 3.1 Pressure Distribution

The pressure distribution over the surfaces of the blades were measured at every  $10^\circ$  interval of the rotor angle between  $0^\circ \leq \alpha \leq 50^\circ$ .



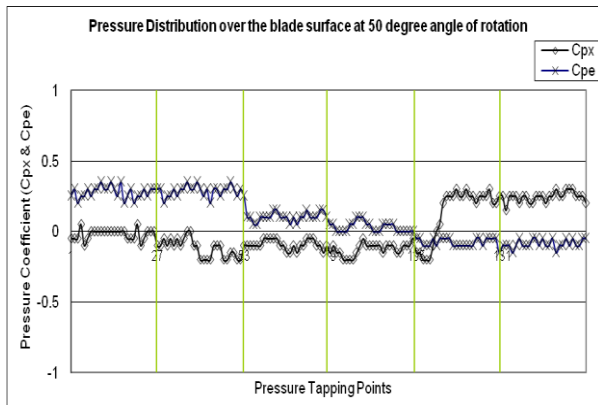


Fig 4. Pressure distribution over the blade surfaces at various rotor angles

### 3.2 Normal Drag Coefficient

Normal drag coefficient,  $C_n$  of an individual blade effect and combined effect of six bladed vane rotor for different rotor angles is shown below:

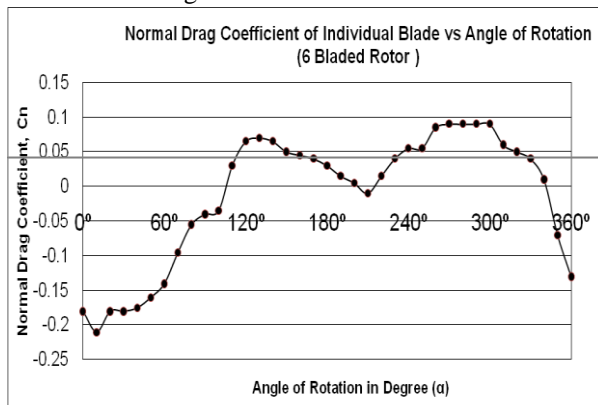
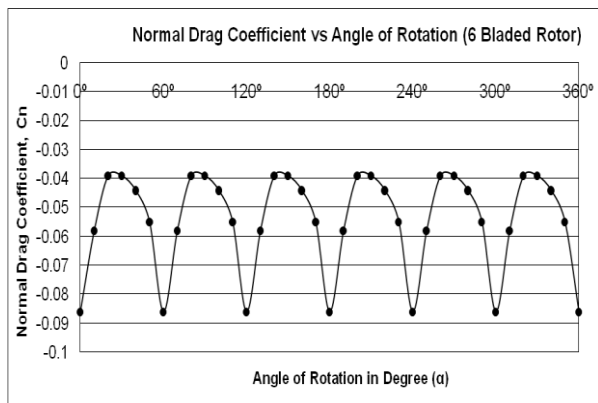


Fig 5(a). Normal Drag Coefficient with the Individual



blade effect (for 6 bladed rotor)

Figure 5(b). Normal Drag Coefficient with the Combined blade effect (for 6 bladed rotor)

### 3.3 Tangential Drag Coefficient

Tangential drag coefficient,  $C_t$  of an individual blade effect and combined effect of six bladed vane rotor for different rotor angles is shown below:

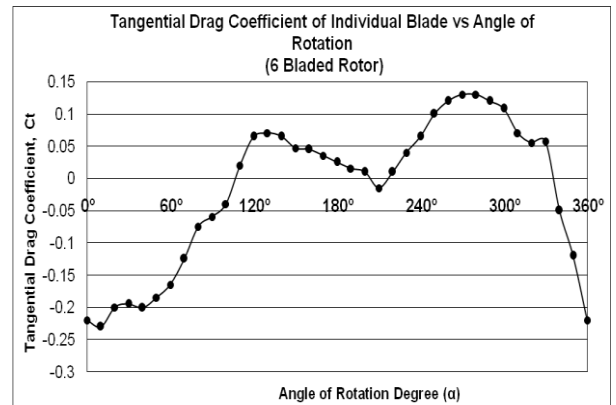


Fig 6(a). Tangential Drag Coefficient with the Individual blade effect (for 6 bladed rotor)

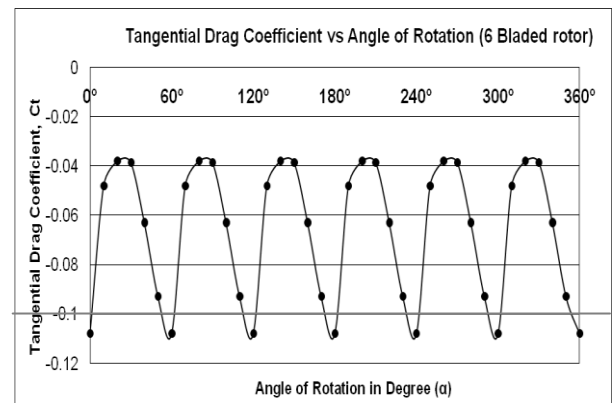


Fig 6(b). Tangential Drag Coefficient with the combined blade effect (for 6 bladed rotor)

### 3.4 Torque Coefficient

Torque coefficient,  $C_q$  with individual blade effect and combined blade effect of six bladed vane rotor is shown below for different rotor angles.

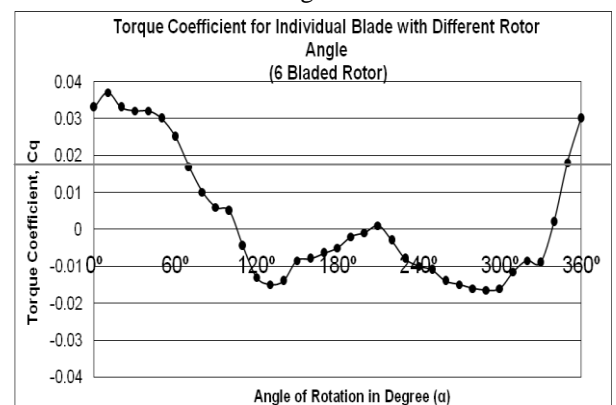


Fig 7(a) Torque Coefficient with the Individual blade effect (for 6 bladed rotor)

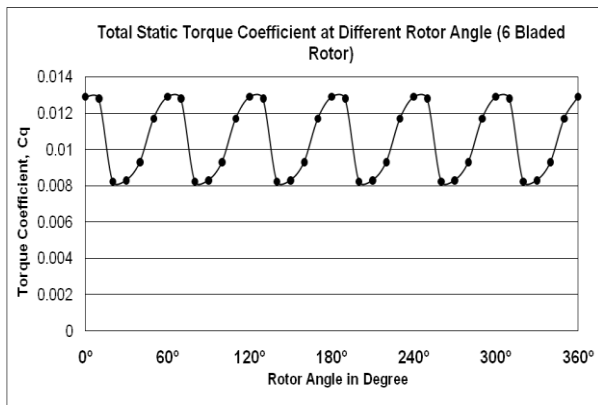


Fig 7(b). Torque Coefficient with the combined blade effect (for 6 bladed rotor)

### 3.5 Power Coefficient

The predicted power coefficients for different tip speed ratios are shown in figure below:

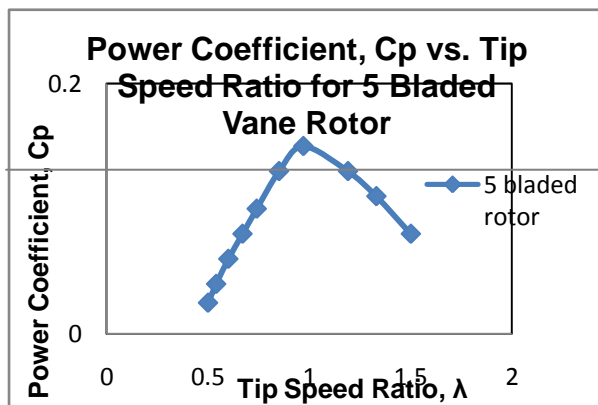


Fig 8. Power Coefficient vs. Tip Speed Ratio curve for 6 bladed vane rotor

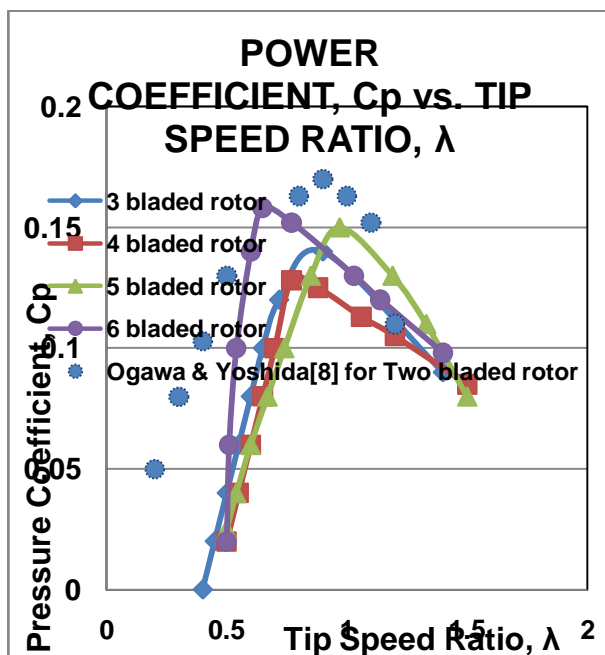


Fig 9. Comparison of Power Coefficient vs. Tip Speed

Ratio curve for different type of rotor

## 4. CONCLUSIONS

In the dynamic part of this research work, the power coefficient ( $C_p$ ) was calculated using the value of the component of relative velocity  $V_w$ , along the free stream velocity  $U_o$ , and the static normal drag coefficient  $C_n$  for different tip speed ratio,  $\lambda$ . From the study, and results of this research work, the following conclusions can be made:

1. It is concluded from the present work that flow separation takes place over the convex and concave surfaces of the blade and location of such separation point depends on the rotor angle.
2. The nature of the torque coefficient is opposite to that of the normal drag coefficient on the individual blade of the bladed vane type rotor. This contributes significantly for producing torque. The value of torque coefficient is smaller than that of normal drag coefficient experienced with individual blade.
3. Total static torque coefficients for six bladed Savonius rotor at different rotor angle were analyzed in the present research work. In this case, it is found that the curve repeats after  $50^\circ$  angle of rotation like that of the normal drag coefficient due to combined effect. And the value of torque coefficient is smaller than that of normal drag coefficient as a result of the combined effect. The torque is always positive for six bladed Savonius rotor.
4. It is concluded from the performance graph of the present study that six bladed vane type rotor provides more power than comparatively other two, three, four and five bladed vane type rotor. In other words, more blades meant more power. However, there is an optimum limit depending on the diameter of the rotor, and size and shape of the blades, etc.
5. For study of dynamic characteristics, the measured power coefficients ( $C_p$ ) for different tip speed ratio ( $\lambda$ ) of the present research work matches with the nature of the theoretical  $C_p$  vs.  $\lambda$  curve. Comparing with the existing measured data, present study agrees well with the curve of the research works. By comparing with the previous existing work and present predicted research work it is observed that the increase in the number of blades makes the nature of the  $C_p$  vs.  $\lambda$  curve steeper. Thus it can be concluded that by increasing the number of blades, the power output can also be increased.

## 5. REFERENCES

1. Lysen, E.H., Bos, H.G. and Cordes, E.H.(1978) , "Savonius Rotor for Water Pumping" SWD Publication, Amersfoort, The Nederland.
2. Beurkens, H.,J.M. (1980), "Low Speed Water Pumping Wind Mills: Rotor Tests and overall performance", Proc. Of 3ed Int. Symp. On Wind Energy System, Copenhagen, Denmark.
3. Park, J.(1975), "Simplified Wind Power for Experimentary" Helion In., California, USA.
4. Sivasegaram, S. (1977), "Design Parameters Affecting the Performance of Resistance Type Rotors", Wind Engineering vol.1,pp.207-217
5. Newman, B.G.. (1974), "Measurements on a Savonius Rotor With a Variable Gap", Proc.

Symposium on Wind Energy: Achievements and Potential, Sherbrooke, Canada.

6. Lysen, E.H. (1983), "Introduction to Wind Energy", Steering Committee of Wind Energy for Developing Countries, P.O. Box 85, Amersfoort, the Nederland.
7. Wilson, R.E., S.N. Walker (1981), "Performance Analysis Program for Propeller Type Wind Turbines" Oregon States University, March, USA.
8. Ogawa, T. and H. Yoshida (1986), "The Effects of Deflecting Plate and Rotor Plate" Bull. JSME, vol. 29, pp. 2115-2121.

## 6. NOMENCLATURE

Symbol	Meaning	Unit
a	Overlap distance	(m)
$C_P$	Power Coefficient	(dimensionless)
$C_{pe}$	Pressure coefficient for concave surface of the blade	(dimensionless)
$C_{px}$	Pressure coefficient for convex surface of the blade	(dimensionless)
$C_t$	Drag coefficient in the transverse direction of the chord	(dimensionless)
$C_q$	Static torque coefficient for a single blade	(dimensionless)
$C_Q$	Total static torque coefficient diameter of blade	(dimensionless)
d	diameter of blade	(m)
D	diameter of the rotor	(m)
$F_n$	Normal force acting on a blade	(N)

$F_t$	Tangential force acting on ablade	(N)
H	Height of rotor	(m)
P	Pressure on blade	(N/m <sup>2</sup> )
$P_a$	Atmospheric pressure	(N/m <sup>2</sup> )
$U_o$	Free stream velocity	(m/s)
T	Static torque on a blade	(Nm/s)
$V_r$	Relative velocity	(m/s)
$\nu$	Kinematic velocity of air	(m <sup>2</sup> /s)
$\omega$	Angular speed of the rotor	(rad/s)
$Re$	Reynolds number, $U_o D / \nu$	(dimensionless)
S	Ratio of overlap distance to diameter of blade	(dimensionless)
$\lambda$	tip speed ratio	(dimensionless)
$\alpha$	Rotor angle	(degree)
$\varphi$	Angle of the pressure tappings	(degree)
$\Delta P$	Difference of pressure between concave and convex surfaces of a blade	(N/m <sup>2</sup> )

## 7. MAILING ADDRESS

**Shamsun Nahar**

Mechanical Engineering Department, Bangladesh University of Engineering and Technology (BUET)

**E-mail:** nahar\_306@yahoo.com